Radiation Damage Monitoring in the ATLAS Pixel Detector

Sally Seidel, on behalf of the ATLAS Collaboration[a,*]

[a] *Department of Physics and Astronomy, University of New Mexico, Albuquerque, NM 87131, USA*

Abstract

We describe the implementation of radiation damage monitoring using measurement of leakage current in the ATLAS silicon pixel sensors. The dependence of the leakage current upon the integrated luminosity is presented. The measurement of the radiation damage corresponding to an integrated luminosity 5.6 fb^{-1} is presented along with a comparison to a model.

PACS: 07.77-n; 29.40-n

Keywords: LHC; pixel; radiation damage; silicon

1. Introduction

The innermost detection system of the ATLAS Detector [1] at the Large Hadron Collider is an n^+-on-n silicon pixel-based tracking and vertexing detector configured in 3 cylindrical barrels and 2×3 endcap disks, spanning $|\eta| < 2.5$. The proximity of the detector to the interaction region (the innermost layer, called Layer 0, has radius 50.5 mm; the outermost, 149.6 mm) implies a harsh radiation environment. Radiation damage incurred by silicon in the pixel region is primarily due to displacement damage and other point defects caused by non-ionizing energy loss of charged particles. Damage-induced recombination or generation centers increase the reverse leakage current, leading to increased power consumption and degrading the signal-to-noise ratio. Charge trapping centers diminish charge collection efficiency, resulting in diminished hit efficiency and track resolution. Acceptor centers change the effective doping concentration, causing the depletion voltage to increase and ultimately leading to type inversion. The innermost layer of this silicon system is expected to undergo type inversion after about 10 fb^{-1} of collision data have been received [2]. To allow experimenters to respond to these changes, the radiation damage sustained by detector elements must be monitored.

Radiation-induced change ΔI in silicon sensor leakage current has been shown to vary directly with fluence $\Phi_{\rm eq}$ through $\Delta I = \alpha \Phi_{\rm eq} V$ [3], where V is the sensor instrumented (depleted) volume (incorporating sensor pattern variations including “long” or “ordinary” pixels, ganged, inter-ganged, and long-inter-ganged pixels, and excluding the guard ring) and α is a temperature-dependent universal constant for silicon with value $(3.99 \pm 0.03) \times 10^{-17}$ A/cm at 20° C after 80 minutes’ annealing at 60° C. For convenience of comparison, fluences of various particle species and energies are typically converted to the fluence of 1 MeV neutrons that would produce an equivalent amount of displacement damage; this is the $\Phi_{\rm eq}$.

A system has been implemented to measure the leakage current in a representative sample of ATLAS Pixel Detector sensors to infer in real time the radiation profile received by the detector. Results presented here were measured for an integrated luminosity of approximately 5.6 fb^{-1} delivered during 2010-11. The sensors have an active thickness (i.e., excluding passivation) of 250.6 ± 0.3 μm and have 46080 channels with pixel granularity 50×400 μm^2. They are combined with their readout electronics into 1744 nearly identical modules. During the period described here, the average operational temperature was maintained at $-13°$ C through evaporative cooling, except during a few documented cooling interruptions. The intrinsic resolution of the Pixel Detector, which includes approximately 80 million channels, is 10 μm in $r\phi$ and 115 μm in rz. All sensors used for this measurement are operated at voltages significantly above full depletion voltage, and all demonstrate pure reverse-bias diode characteristics. The starting bias voltage for

*Corresponding author. e-mail: seidel@phys.unm.edu

each device is 150 V. The Pixel Detector inner layer is designed to tolerate a radiation dose of 500 kGy or 10^{15} 1 MeV n_{eq} cm^{-2}.

2. Sensor Current Monitoring in the ATLAS Pixel Detector

High Voltage Patch Panel 4 (HVPP4), located in the ATLAS detector cavern, distributes sensor bias voltage to the ATLAS Pixel Detector. The pixels use power supplies produced by ISEG GmbH, which can distribute power at voltage V_{DC} up to 700 V and current $I \leq$ 4mA. When the leakage current is low, each ISEG unit supplies six or seven pixel modules. The modularity will be reconfigured to 1 ISEG supply per 2-3 detector modules as currents rise.

The Current Measurement (CM) system monitors the leakage current on individual pixel modules. To assure precision results throughout the lifetime of the Pixel Detector, and from representative sensors installed in all layers, the system must measure currents over the range 0.01 μA to 1 mA. Figures 1 and 2 show the circuit diagram and a photograph of its implementation. A current-frequency converter circuit is optically coupled to a frequency-voltage converter. Two digital readout ranges are available per channel, with different analog gains. Four circuits per board monitor selected modules through the radiation hard 64-channel Embedded Local Monitor Board (ELMB) [4]. The high gain channel reads out module leakage currents in the range 10^{-8} to 10^{-5} A, and the low gain channel, in the range 10^{-6} to 10^{-2} A. The output voltage range is fixed by the standard ELMB input ranges; at the outset of the run, the range $0-1$ V was chosen. This will be changed to the $0-5$ V range as the high gain channels saturate at pixel leakage currents above about 10^{-5} A. Channels are isolated in pairs from each other and from the readout system. The frequency of the operating circuit is less than 100 kHz. The measured current values are digitized and transmitted from the CM board (which is attached to the HVPP4 Type II board) via CANbus to the Detector Control System (DCS) by the 16-bit analog-to-digital converter ELMB. PVSS software reads the data from the ELMB and downloads it to the DCS offline PVSS Archive Database. The resolution of the CM system is (ELMB range)/2^{16}, implying a current measurement precision approaching 10 nA. Noise is negligible in this regime. The CM system comprises 22 boards for Layer 0, 16 boards for Layer 1, and 16 boards for Layer 2, and by reading out 4 modules per board, samples 216 barrel modules uniformly in η and ϕ.

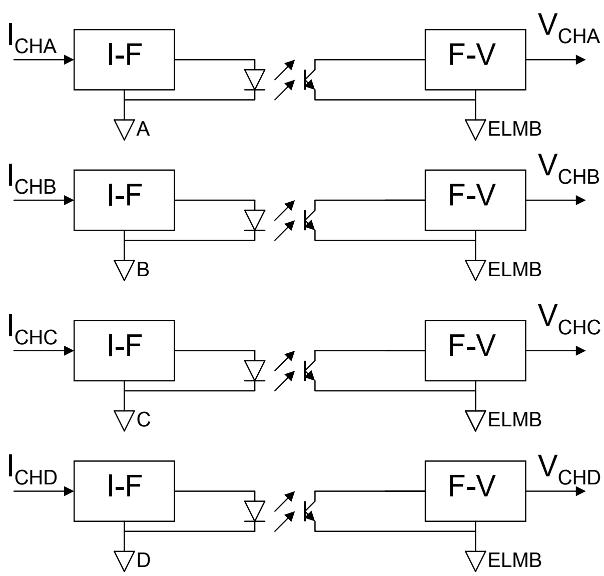

Figure 1: The Current Measurement circuit. A, B, C, and D are the independent grounds of the four modules.

Figure 3 shows the two available ranges of output voltage versus input current that are available with this system. The system input calibration is made with a Keithley 237 High Voltage Source/Measure Unit in constant current mode. The calibration output voltage is measured through the ELMB with PVSS. Temperatures are read out and time

Figure 2: A sample Current Measurement Board.

stamped continuously by NTC sensors mounted directly on the modules, as close as possible to the silicon sensors. The impact of the difference between the temperature at the module mounting point and the temperature of the silicon is under study.

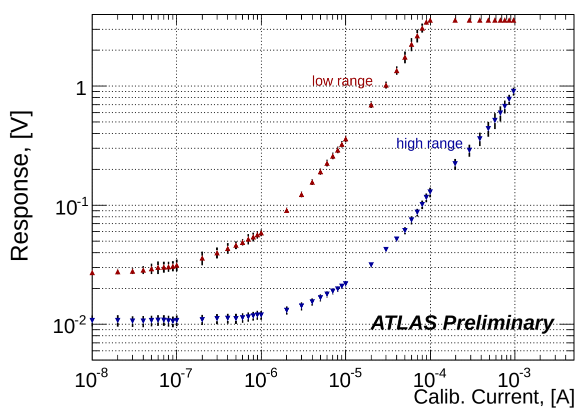

Figure 3: Output voltage versus input current to a representative board in the Current Measurement system. The high and low gain ranges are evident.

3. Comparison of Data to the Model

Fluences at various points in the ATLAS Inner Detector have been predicted[2] for radii between 2 and 20 cm of the proton-proton collisions using the ATLAS Monte Carlo simulation with packages PHOJET and FLUKA [5]. The response, including annealing, of silicon to particle interactions has been modeled [6, 7]. The simulation includes neutron backscatter from the calorimeter as well as charged particles from the interaction. Predictions with GEANT4 are under development.

Data are taken every 30 seconds. For the comparison, recorded currents are corrected for pedestal current and scaled to 0°C by the formula $I(T_{\mathrm{ref}}) = I(T)\left(\frac{T_{\mathrm{ref}}}{T}\right)^2 exp\left[-\frac{E_g}{2k_B}\left(\frac{1}{T_{\mathrm{ref}}} - \frac{1}{T}\right)\right]$. Here E_g is the effective silicon band gap, 1.21 eV [8], and k_{B} is the Boltzmann constant. Correction for beam-induced ionization current is made by subtracting $I_{\mathrm{hit}} = N_{\mathrm{b}} \cdot \nu_{\mathrm{LHC}} \cdot Occ \cdot C_{\mathrm{hit}}$, where N_{B} is the number of colliding bunches per train (this increased throughout the period examined, with a maximum of about 1330 at the end of 2011); ν_{LHC} is the LHC revolution frequency (value approximately 1.4×10^8 sec^{-1}); Occ is the pixel hit occupancy per module (typically 10^{-6}), and C_{hit} is the deposited charge per hit (of mean value 20,000 electrons). Beam induced current is comparable to leakage current in unirradiated detectors and rapidly becomes negligible as the detectors are irradiated. As the Pixel Detector bias voltage is put to zero when beam is off, volume leakage current is recorded only when beam is on. The contribution of surface currents is presently under study but expected to be small and known to saturate at high fluence.

Figure 4 shows the corrected leakage current in Pixel barrel Layer 0 as a function of integrated luminosity. The prediction of the model is superimposed. The agreement is good, and the annealing periods are prominent. The approximately linear correlation with integrated luminosity confirms that the fluence is dominated by proton-proton collisions.

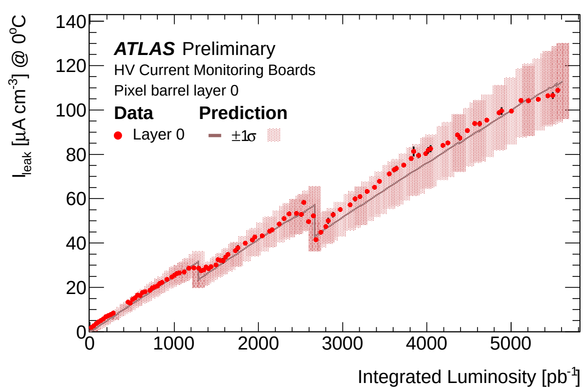

Figure 4: Points indicate measured corrected leakage current at Layer 0 as a function of integrated luminosity. The prediction by the model [7] is also shown. The discontinuities reflect annealing that occurred when the beam was off. The primary source of uncertainty in the model is knowledge of the slowest annealing component.

4. Conclusions and Outlook

Leakage currents measured in the ATLAS Pixel Detector's Layer 0 have been compared to a model and found to agree well for proton-proton collision integrated luminosity up to 5.6 pb^{-1}. This information can be used to validate the ATLAS simulation model, which includes charge trapping, electric field modification, and signal induction on the electrodes, and make predictions about the response of LHC detectors to future operation scenarios.

References

[1] ATLAS Collaboration, JINST 3, S08003 (2008).
[2] ATLAS Radiation Background Task Force, ATL-GEN-2005-001 (2005). Information about the conversion of fluence to NIEL, and related uncertainties, may be found at pages 73-74 and 100.
[3] M. Moll et al. [CERN-ROSE/RD48 Collaboration], Nucl. Instr. and Meth. A 426, 87 (1999).
[4] Embedded Local Monitor Board ELMB128, http://elmb.web.cern.ch/ELMB/elmb128_1.pdf.
[5] R.S. Harper, Nucl. Instr. and Meth. A 479, 548-554 (2002).
[6] M. Moll, Hamburg University Ph.D. dissertation, 1999 (unpublished).
[7] O. Krasel, Dortmund University Ph.D. dissertation, 2004 (unpublished).
[8] A. Chilingarov, RD50 Technical Note RD50-2011-1.